

## Numerical Simulation of Influence of Reduced Electric Fields on NO<sub>x</sub> Removal in N<sub>2</sub>/O<sub>2</sub>/H<sub>2</sub>O/CO<sub>2</sub> Mixture

Rida AHMED AMMAR\* and Mostefa LEMERINI

Theoretical Physics Laboratory, Department of Physics, Faculty of Sciences, University of Tlemcen, Tlemcen (13000), Algeria

Received 27 May 2017; Accepted 16 September 2017

### Abstract

The aim of this work is to investigate the time evolution of various species concerned in N<sub>2</sub>/O<sub>2</sub>/H<sub>2</sub>O/CO<sub>2</sub> mixed gas induced by negative corona discharge at atmospheric pressure. This study takes under consideration thirty totally different chemical species taking part in two hundred selected chemical reactions. The density is analyzed by the continuity equation without the diffusion term. In literature it has generally been emphasized that certain radicals N, O, and O<sub>3</sub> influence the NO or NO<sub>2</sub> removal. In this work we complete these studies by analyzing others species such as negative ions O<sub>2</sub><sup>-</sup>, O<sub>3</sub><sup>-</sup>, O<sub>4</sub><sup>-</sup> and radicals OH, HO<sub>2</sub> presents in N<sub>2</sub>/O<sub>2</sub>/H<sub>2</sub>O/CO<sub>2</sub> mixture which they participate in NO<sub>x</sub> removal. In particular, we tend to analyze the time evolution (10<sup>-9</sup>-10<sup>-3</sup> s) of depopulation rate and rate coefficient of bound reactions, beneath completely different reduced electrical fields within the vary of 100-200 Td (1Td=10<sup>-21</sup> V.m<sup>2</sup>). The results show that the environmental condition rate of NO, NO<sub>2</sub> and NO<sub>3</sub> is well affected by the increase of reduced electric field and concentration.

**Keywords:** Rate coefficient, NO<sub>x</sub> removal, chemical kinetic, corona discharge, reduced electric field

### 1. Introduction

Gas discharge plasmas are able to initiate chemical reactions in normally inert gas mixtures [1]. The common thermal and catalytic techniques used for many years to remove the NO<sub>x</sub> and SO<sub>x</sub> present in industrial flue gas or emitted by the vehicles will not permit us to respect the new emission limits which become more and more severe to protect the environment. These effects may also have an immediate impact on the targeted applications like electron beam processes that were significantly studied for treatment of gaseous effluents impure by nitrogen oxides, sulphur [2-4] and/ or ozone production [5-8], medical applications [9-13] and surface treatment [14-15]. Thus, new more efficient depolluting processes are at present studied and the use of non-thermal plasmas created by electron beam or electrical discharge methods [16-22] appears very attractive. The energetic electrons created by the discharge strike the background gas molecules, thereby making long atomic and molecular free radicals that move with the pollutants and convert them, throughout the post-discharge, into clean or easier to gather product through a fancy set of physical and chemical reactions. many previous studies have already shown the result of non-equilibrium discharges gas dynamics at atmospheric pressure [23-26]. These effects can be dynamic (collective movement of drift) and/or thermal (correlated movements) by nature. The charged particles, notably the ions, can transfer a section of their derivative movement to the neutralones. The motion of a fluid induced

by an electrical discharge is cited as an electrical wind or ion wind. It was demonstrated long ago and widely studied in the case of a corona discharge between a tip and a plane [27-30]. Generally, the charged particles created in the inter electrode space are accelerated by the electric field E. It is well known that all electrical proprieties are depending on the reduced field E/N, where N is the density of neutral gas and E the electric field [31-33], and increase the internal energy of the neutral gas. During the section of post-discharge, the undulation energy reservoir bit by bit relaxes causings light-weight warming of the ionising channel and an area reduction within the gas density. The chemical reactivity of the neutral gas mixture permits transformation of the toxic molecule into harmless particles (such as N<sub>2</sub>O or N) or to form acids (such as the nitric acid) within the plasma.

These acids can be transformed into salt (by addition of a base) [34-36]. In this way, the aim of the present study is to simulate for different values of reduced electric field (100 - 200 Td), the time evolution of thirty chemical species (electrons e, molecules N<sub>2</sub>, O<sub>2</sub>, H<sub>2</sub>O, CO<sub>2</sub>, OH, HO<sub>2</sub>, HNO<sub>3</sub>, H<sub>2</sub>, CO, O<sub>3</sub>, atoms N, O, H, nitric oxides NO, N<sub>2</sub>O, NO<sub>2</sub>, NO<sub>3</sub>, N<sub>2</sub>O<sub>5</sub>, positive ions (NO<sup>+</sup>, N<sub>2</sub><sup>+</sup>, O<sub>2</sub><sup>+</sup>), negative ions (O<sup>-</sup>, O<sub>2</sub><sup>-</sup>, O<sub>3</sub><sup>-</sup>, O<sub>4</sub><sup>-</sup>, NO<sub>2</sub><sup>-</sup>, NO<sub>3</sub><sup>-</sup>) and metastables species N(<sup>2</sup>D), O(<sup>1</sup>D), in the mixture (N<sub>2</sub>: 78%, O<sub>2</sub>: 18%, H<sub>2</sub>O: 2% and CO<sub>2</sub>: 2%). These different species react following 200 selected chemical reactions. In this numerical simulation we suppose various effects induced by the passage of a corona discharge in a mixed gas. Processing Re-write Suggestions Done (Unique Article) For the sake of simplification, we tend to assume that the gas has no convective movement gradients and also the pressure remains constant.

\*E-mail address: rammar31@yahoo.com

ISSN: 1791-2377 © 2017 Eastern Macedonia and Thrace Institute of Technology. All rights reserved.

doi:10.25103/jestr.104.07

2. Mathematical Model

The mathematical model utilized in this work consists of a system of equations that takes under consideration the variation of the density and also the chemical kinetics of the environment. We developed a zero order numerical code to resolve the transport equations for neutral and charged particles. The algorithm is based on the time integration of the system of equations under consideration the variation of the density and the chemical kinetics of the environment. The chemical kinetics equation systems is delineate by an ordinary differential equation system that has the subsequent form:

$$\frac{dN_i}{dt} = \sum_{j=1}^{j_{max}} Q_{ij} \quad \text{where } j = 1, \dots, j_{max} \quad (1)$$

where:

$$Q_{ij} = (G_{ij} - L_{ij}) \quad (2)$$

$N_i$  represent the vector of all species densities,  $i=1$  up to 30 considered in the plasma and  $Q_{ij}$  the source term vector depending on the reaction coefficients and corresponding to the contributions from different processes.  $G_{ij}$  and  $L_{ij}$  represent respectively the gain and loss of species  $i$  due to the chemical reactions  $j=1$  up to  $j_{max}=200$ . The solution of such a system needs the information of the initial

concentrations. The total density  $N$  of the gas is given by the ideal gas law:

$$P=Nk_b T \quad (3)$$

Where  $P$  represents the pressure,  $k_b$  Boltzmann constant and  $T$  the absolute temperature. The reactivity of the gas is taken into account in the source term  $Q_{ij}$  of the density conservation Eq. (1).

$$G_{ij} = \sum_{\alpha} K_{\alpha}(T)(n_i n_j)_{\alpha} \quad (4)$$

$$L_{ij} = \sum_{\beta} K_{\beta}(T)(n_i n_j)_{\beta} \quad (5)$$

$K_{\alpha}(T)$  and  $K_{\beta}(T)$  are the coefficients of the chemical reaction number  $\alpha$  or  $\beta$  and  $(n_i n_j)$  is the product of densities of species  $i$  and  $j$  interacting in response to the reaction  $\alpha$  or  $\beta$ . These coefficients satisfies Arrhenius formula:

$$K_{\alpha}(T) = A. \exp\left(\frac{-\theta_{\alpha}}{T}\right) \quad (6)$$

$$K_{\beta}(T) = B. \exp\left(\frac{-\theta_{\beta}}{T}\right) \quad (7)$$

Where  $A$  and  $B$  are the constants factor and  $\theta_{\alpha}$  and  $\theta_{\beta}$  are the activation energy of the reaction and  $T$  the absolute temperature of the species involved in the warm rain that has left the chemical reaction.

**Table 1** The main plasma reactions to generate the main radical to remove NOx and their rate constants. (Rate constants are in units of  $\text{cm}^3 \cdot \text{molecule}^{-1} \cdot \text{s}^{-1}$  for two body reactions, and  $\text{cm}^6 \cdot \text{molecule}^{-2} \cdot \text{s}^{-1}$  for three body reactions.  $T$  is the gas temperature in Kelvin).

	Reactions	Rate constants	Ref.
R1	$O_2 + e \rightarrow O + O + e$	$k_1 = 15 \times 10^{-9}$	[37]
R2	$O_2 + e \rightarrow O + O(^1D) + e$	$k_2 = 5.25 \times 10^{-9}$	[37]
R3	$N_2 + e \rightarrow N + N + e$	$k_3 = 2.05 \times 10^{-11}$	[38]
R4	$H_2O + e \rightarrow OH + H + e$	$k_4 = 3.35 \times 10^{-10}$	[39]
R5	$CO_2 + e \rightarrow CO + O + e$	$k_5 = 8.7 \times 10^{-11}$	[40]
R6	$O + O_2 + N_2 \rightarrow O_3 + N_2$	$k_6 = 6.2 \times 10^{-34}$	[27]
R7	$O + O_2 + O_2 \rightarrow O_3 + O_2$	$k_7 = 6.9 \times 10^{-34}$	[27]
R8	$O_3 + OH \rightarrow HO_2 + O_2$	$k_8 = 6.4 \times 10^{-14}$	[27]
R9	$N + O + N_2 \rightarrow NO + N_2$	$k_9 = 1.76 \times 10^{-31} \times T^{-0.5}$	[34]
R10	$N + O + O_2 \rightarrow NO + O_2$	$k_{10} = 1.76 \times 10^{-31} \times T^{-0.5}$	[34]
R11	$N + N + N_2 \rightarrow N_2 + N_2$	$k_{11} = 8.3 \times 10^{-34}$	[35]
R12	$N + O_2 \rightarrow O + NO$	$k_{12} = 8.9 \times 10^{-17}$	[27]
R13	$N + NO_2 \rightarrow NO + NO$	$k_{13} = 2.3 \times 10^{-12}$	[34]
R14	$N + NO \rightarrow O + N_2$	$k_{14} = 3 \times 10^{-11}$	[34]
R15	$N + O_2 \rightarrow O + NO$	$k_{15} = 8.9 \times 10^{-17}$	[27]
R16	$N + NO_2 \rightarrow N_2 + O_2$	$k_{16} = 7 \times 10^{-13}$	[34]
R17	$NO + NO_3 \rightarrow NO_2 + NO_2$	$k_{17} = 2 \times 10^{-11}$	[27]
R18	$NO + NO_3 \rightarrow NO_2 + NO_2$	$k_{18} = 2 \times 10^{-11}$	[27]
R19	$NO + NO_3 \rightarrow NO_2 + NO_2$	$k_{19} = 2 \times 10^{-11}$	[27]
R20	$NO + O_3 \rightarrow O_2 + NO_2$	$k_{20} = 1.8 \times 10^{-12}$	[35]
R21	$O_2^- + NO_2 \rightarrow NO_2^- + O_2$	$k_{21} = 7.0 \times 10^{-10}$	[41]
R22	$O_3^- + NO \rightarrow NO_2^- + O_2$	$k_{22} = 2.0 \times 10^{-12}$	[41]
R23	$O_3^- + NO \rightarrow NO_3^- + O$	$k_{23} = 1.0 \times 10^{-10}$	[41]
R24	$O_3^- + N \rightarrow NO + O_2 + e$	$k_{24} = 5.0 \times 10^{-10}$	[41]
R25	$O_3^- + NO_2 \rightarrow NO_2^- + O_3$	$k_{25} = 7 \times 10^{-10}$	[34]
R26	$O_3^- + NO_2 \rightarrow NO_3^- + O_2$	$k_{26} = 2 \times 10^{-11}$	[34]
R27	$O_3^- + NO_3 \rightarrow NO_3^- + O_3$	$k_{27} = 5.0 \times 10^{-10}$	[34]
R28	$O_4^- + NO \rightarrow NO_3^- + O_2$	$k_{28} = 2.5 \times 10^{-10}$	[41]
R29	$NO_2 + O_3 \rightarrow O_2 + NO_3$	$k_{29} = 1.2 \times 10^{-13} \exp(-2450/T)$	[34]

R30	$\text{NO}_2 + \text{NO}_3 + \text{N}_2 \rightarrow \text{N}_2\text{O}_5 + \text{N}_2$	$k_{30} = 1.01 \times 10^{-27}$	[35]
R31	$\text{NO}_2 + \text{NO}_3 + \text{O}_2 \rightarrow \text{N}_2\text{O}_5 + \text{O}_2$	$k_{31} = 1.01 \times 10^{-27}$	[35]
R32	$\text{NO}_2 + \text{N} \rightarrow \text{N}_2 + \text{O}_2$	$k_{32} = 7 \times 10^{-13}$	[34]
R33	$\text{NO}_2 + \text{O}_3 \rightarrow \text{O}_2 + \text{NO}_3$	$k_{33} = 1.2 \times 10^{-13} \exp(-2450/T)$	[34]
R34	$\text{NO}_2 + \text{NO}_3 \rightarrow \text{N}_2\text{O}_5$	$k_{34} = 1.1 \times 10^{-12}$	[27]
R35	$\text{NO}_3 + \text{HO}_2 \rightarrow \text{HNO}_3 + \text{O}_2$	$k_{35} = 4.05 \times 10^{-12}$	[40]
R36	$\text{NO}_3 + \text{NO}_3 \rightarrow \text{O}_2 + \text{NO}_2 + \text{NO}_2$	$k_{36} = 1.2 \times 10^{-15}$	[27]
R37	$\text{OH} + \text{NO}_2 \rightarrow \text{HNO}_3$	$k_{37} = 13.5 \times 10^{-11}$	[41]
R38	$\text{OH} + \text{NO}_3 \rightarrow \text{HO}_2 + \text{NO}_2$	$k_{38} = 2.35 \times 10^{-11}$	[41]
R39	$\text{NO}_3^- + \text{N} \rightarrow \text{NO} + \text{NO}_2 + \text{e}$	$k_{39} = 5.0 \times 10^{-10}$	[41]
R40	$\text{N}_2\text{O}_5 + \text{O}_2 \rightarrow \text{NO}_2 + \text{NO}_3 + \text{O}_2$	$k_{40} = 1.6 \times 10^{-19}$	[27]
R41	$\text{N} (^2\text{D}) + \text{O}_2 \rightarrow \text{NO} + \text{O}$	$k_{41} = 5.2 \times 10^{-12}$	[40]
R42	$\text{O}_3 + \text{HO}_2 \rightarrow \text{OH} + 2\text{O}_2$	$k_{42} = 1.45 \times 10^{-14} \exp(-600/T)$	[40]
R43	$\text{O}_3 + \text{H} \rightarrow \text{OH} + \text{O}_2$	$k_{43} = 1.45 \times 10^{-14} \exp(-480/T)$	[41]
R44	$\text{HO}_2 + \text{NO} \rightarrow \text{NO}_2 + \text{OH}$	$k_{44} = 13.5 \times 10^{-11}$	[41]
R45	$\text{CO}_2 + \text{N} \rightarrow \text{NO} + \text{CO}$	$k_{45} = 3.2 \times 10^{-13} \exp(-1711/T)$	[41]
R46	$\text{NO}_3^- + \text{O}_2^+ + \text{N}_2 \rightarrow \text{NO}_3 + \text{O}_2 + \text{N}_2$	$k_{46} = 2 \times 10^{-7} \times (300/T)^{0.5}$	[34]

### 3. Results and Discussion

The chemical kinetics involves 30 different chemical species: electrons (e), molecules  $\text{N}_2$ ,  $\text{O}_2$ ,  $\text{H}_2\text{O}$ ,  $\text{CO}_2$ ,  $\text{OH}$ ,  $\text{HO}_2$ ,  $\text{HNO}_3$ ,  $\text{H}_2$ ,  $\text{CO}$ ,  $\text{O}_3$ , atoms  $\text{N}$ ,  $\text{O}$ ,  $\text{H}$ , nitric oxides  $\text{NO}$ ,  $\text{N}_2\text{O}$ ,  $\text{NO}_2$ ,  $\text{NO}_3$ ,  $\text{N}_2\text{O}_5$ , positive ions  $\text{NO}^+$ ,  $\text{N}_2^+$ ,  $\text{O}_2^+$ , negative ions  $\text{O}^-$ ,  $\text{O}_2^-$ ,  $\text{O}_3^-$ ,  $\text{O}_4^-$ ,  $\text{NO}_2^-$ ,  $\text{NO}_3^-$ , metastable species  $\text{N} (^2\text{D})$ ,  $\text{O} (^1\text{D})$ . These different species react following 200 selected chemical reactions the main ones are given in Table 1. In this section we will analyze the effects of oxidizing radicals  $\text{O}_3^-$ ,  $\text{O}_4^-$  and  $\text{HO}_2$  on removing  $\text{NO}$  specie, we calculate in particular the rate coefficient of reactions R22, R23, R28 and R44 between  $10^{-9}$  s and  $10^{-3}$  s. These reactions in this work are the main reactions to remove  $\text{NO}$  specie. Therefore we analyze the effects of oxidizing radicals  $\text{O}_3^-$ ,  $\text{O}_4^-$ , and  $\text{OH}$  on  $\text{NO}_2$ ,  $\text{NO}_3$  species through reactions R25, R26, R27, R37 and R38. According to Table 1, we can say that the  $\text{NO}$  is converted into  $\text{NO}_2$ ,  $\text{NO}_3^-$ ,  $\text{O}$ ,  $\text{O}_2$  and  $\text{OH}$  species via four reactions: R22, R23, R28 and R44.

So, in figures 1 to 4 we have shown the time evolution of rate coefficient of those reactions at numerous values of reduced electrical fields (100, 120, 140, 160, 180 and 200 Td). We notice that  $\text{NO}$  can react with the oxidizing radicals such as  $\text{O}_3^-$ ,  $\text{O}_4^-$  and  $\text{HO}_2$  to form especially  $\text{NO}_2^-$ ,  $\text{NO}_3^-$ ,  $\text{O}$  and  $\text{OH}$ . We note firstly that the effectiveness of these reactions is higher at the beginning than at the end. Secondly, plus the value of the reduced electric field is more important reaction is effective. For example, at 100 Td the rate coefficient does not vary significantly, but at 200 Td we have a significant reduction. We notice to all of these curves that the reactions become less effective after  $t = 3 \times 10^{-4}$  s.

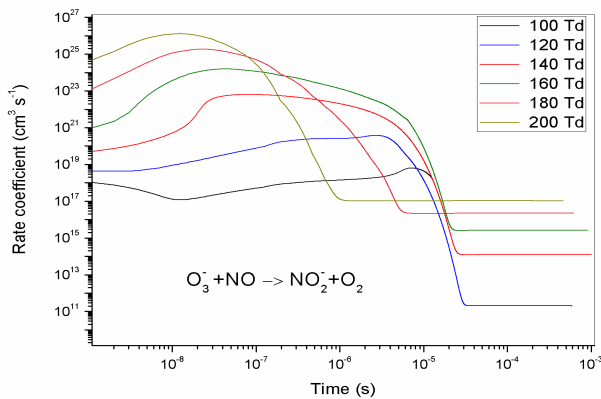


Fig. 1. Time evolution of rate coefficient of reaction R22:  $\text{O}_3^- + \text{NO} \rightarrow \text{NO}_2^- + \text{O}_2$  for different reduced electric fields [100-200 Td]

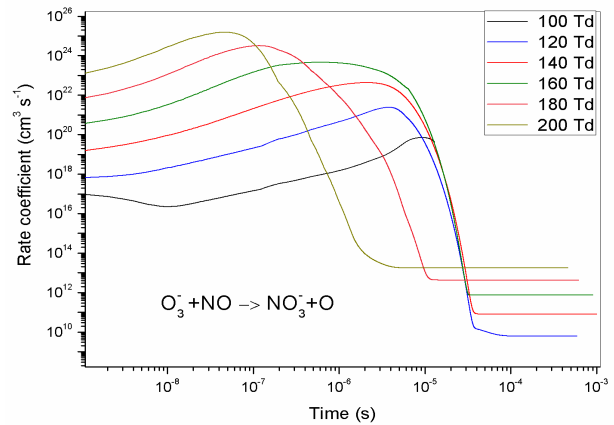


Fig. 2. Time evolution of rate coefficient of reaction R23:  $\text{O}_3^- + \text{NO} \rightarrow \text{NO}_3^- + \text{O}$  for different reduced electric fields [100-200 Td]

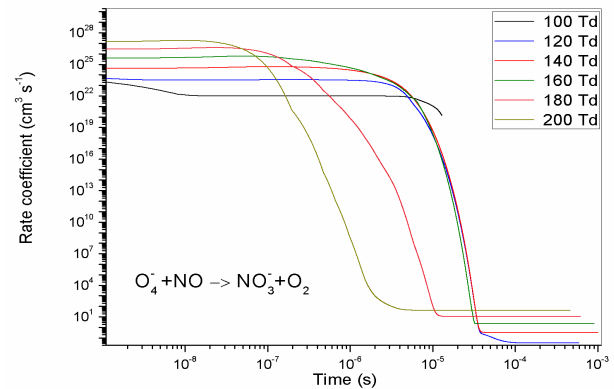


Fig. 3. Time evolution of rate coefficient of reaction R28:  $\text{O}_4^- + \text{NO} \rightarrow \text{NO}_3^- + \text{O}_2$  for different reduced electric fields [100-200 Td]

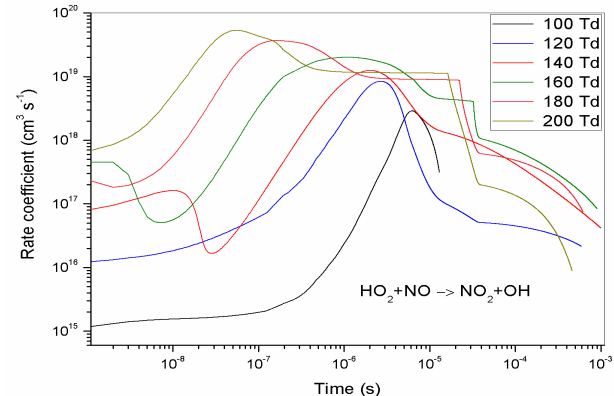


Fig. 4. Time evolution of rate coefficient of reaction R44:  $\text{HO}_2 + \text{NO} \rightarrow \text{NO}_2 + \text{OH}$  for different reduced electric fields [100-200 Td]

Figure 5 shows the time evolution of depopulation rate  $((N_0-N)/N_0)$ , wherever  $N_0$  represents the initial density and  $N$  the density values between  $10^{-9}$  s and  $10^{-3}$  s of NO specie in mixture  $N_2/O_2/H_2O/CO_2$  for various reduced electrical fields (100 - 200 Td). We presented in this figure the results of the competition between all participants reactions to oxide nitrogen reduction. We clearly observe the influence of the reduced electric field on NO reduction. It is noted for low values of the reduced electric field 100 Td and 120 Td an average reduction of 10% caused by the overall reaction, while for high value 180 Td we observed that the rate of reduction reached 70%. Finally, NO reduction (R22, R23, R28 and R44) largely depends on the radical concentration of  $O_3^-$ ,  $O_4^-$  and  $HO_2$ . In the beginning, the NO consumption is not significant because the  $O_3^-$ ,  $O_4^-$  and  $HO_2$  radicals generated react mostly with  $NO_x$  and their concentration remains low.

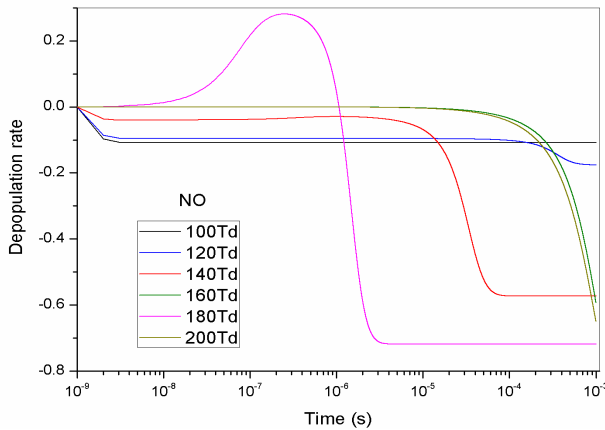


Fig. 5. Time evolution of depopulation rate of NO specie in mixture  $N_2/O_2/H_2O/CO_2$  for different reduced electric fields [100-200 Td]

In the following section, we will analyze the effects of oxidizing radicals  $O_3^-$  and  $OH$  on removing  $NO_2$  and  $NO_3$  species which represent with the oxide nitrogen to the main  $NO_x$ . We calculate in particular like before the rate coefficient of reactions R25, R26, R27, R37 and R38 between  $10^{-9}$  s and  $10^{-3}$  s. According to Table 1, these reactions are the main reactions to remove  $NO_2$  and  $NO_3$  species. We notice that these species react with  $O_3^-$  and  $OH$  to form especially  $O_2$ ,  $O_3$ ,  $NO_2^-$ ,  $NO_3^-$ ,  $HO_2$  and  $HNO_3$ . As for the oxide nitrogen results we notice that the reaction rate shown in figures 6 to 10, is related with the increase of the reduced electric field. Also, we notice to all of these curves on these figures that the reactions become less effective after  $t = 3 \times 10^{-4}$  s except for the reaction R27 where the influence goes up to  $10^{-3}$  s.

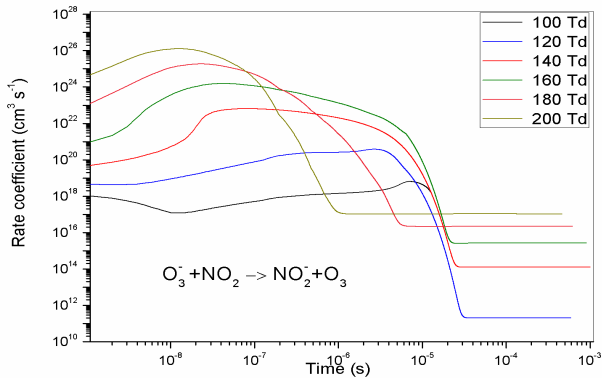


Fig. 6. Time evolution of rate coefficient of reaction R25:  $O_3^- + NO_2 \rightarrow NO_2^- + O_3$  for different reduced electric fields [100-200 Td]

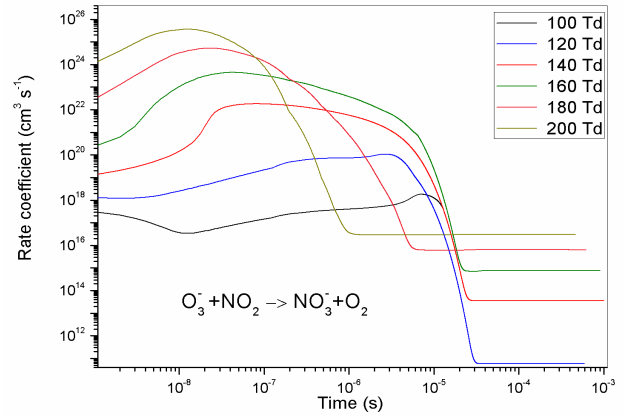


Fig. 7. Time evolution of rate coefficient of reaction R26:  $O_3^- + NO_2 \rightarrow NO_3^- + O_2$  for different reduced electric fields [100-200 Td]

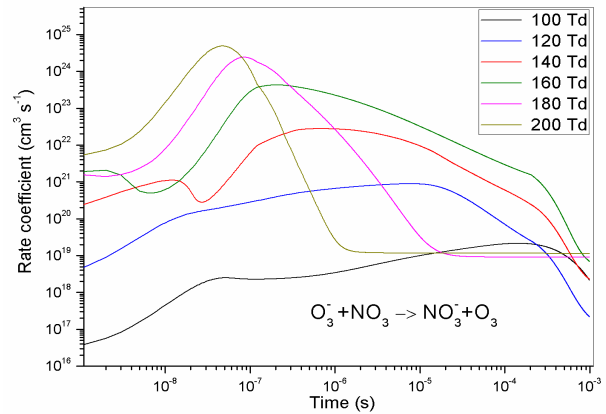


Fig. 8. Time evolution of rate coefficient of reaction R27:  $O_3^- + NO_3 \rightarrow NO_3^- + O_3$  for different reduced electric fields [100-200 Td]

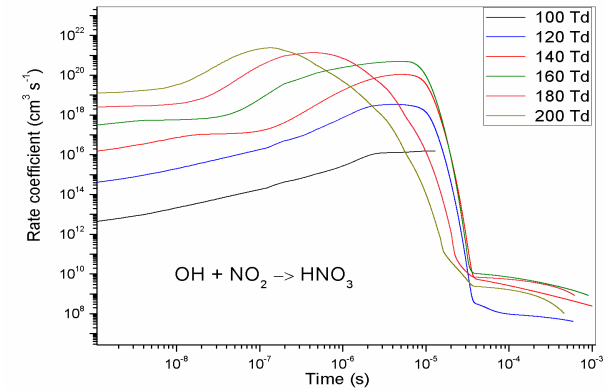


Fig. 9. Time evolution of rate coefficient of reaction R37:  $OH + NO_2 \rightarrow HNO_3$  for different reduced electric fields [100-200 Td]

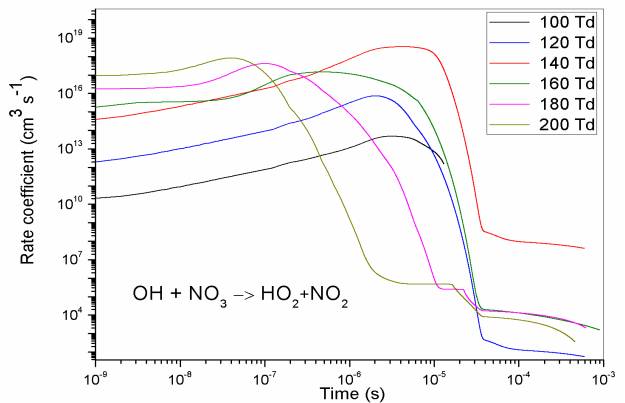


Fig. 10. Time evolution of rate coefficient of reaction R38:  $OH + NO_3 \rightarrow HO_2 + NO_2$  for different reduced electric fields [100-200 Td]

Figure 11 shows the time evolution of depopulation rate of NO<sub>2</sub> for varied values of reduced electrical fields (100 - 200 Td). Unlike the previous result for oxide nitrogen, we observe for NO<sub>2</sub> a different behavior. Firstly, we notice in the beginning from 10<sup>-9</sup> s to 10<sup>-8</sup> s, a significant reduction (80% on average) especially for 100 and 120 Td which stabilizes at this value until the end. Secondly at 140 and 180 Td there is a different behavior, for example when the reduced electric field equals 140 Td the depopulation rate decreases and reaches approximately 20% at 5x10<sup>-8</sup> s. Then there an increase that reached 70% on average at the moment 5x10<sup>-8</sup> s followed by a reduction (25%) till the end.

Figure 12 shows the depopulation rate of NO<sub>3</sub> specie under the same conditions as above. It is noted a creation followed by consumption for 100, 120 and 140 Td. The rate production reached 90% on average for these three values until 10<sup>-7</sup> s, then decreases down to zero till the end of time. We observe unusually for 160 and 200 Td a balance between production and reduction of this species up to 10<sup>-5</sup> s, then the rate decreases. Unlike other values, when the reduced electric field equals 180 Td, the density of NO<sub>3</sub> decreases until 2x10<sup>-8</sup> s and the depopulation rate reaches approximately 75%, then the density increases until 2x10<sup>-7</sup> s where the rate variation exceeds 80%, then the density drops again and the rate reaches 90% and stabilizes at this value.

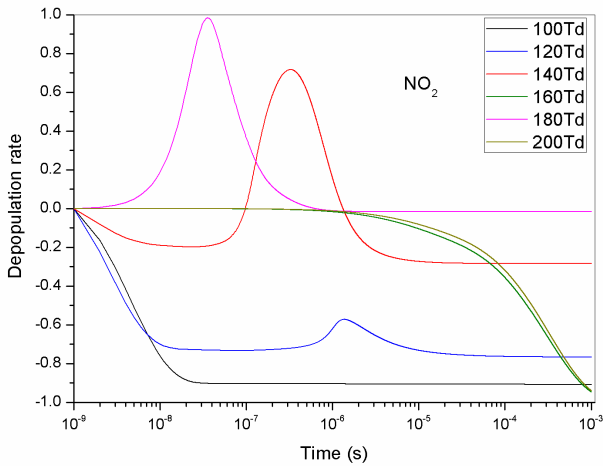


Fig. 11. Time evolution of depopulation rate of NO<sub>2</sub> specie in mixture N<sub>2</sub>/O<sub>2</sub>/H<sub>2</sub>O/CO<sub>2</sub> for different reduced electric fields [100-200 Td]

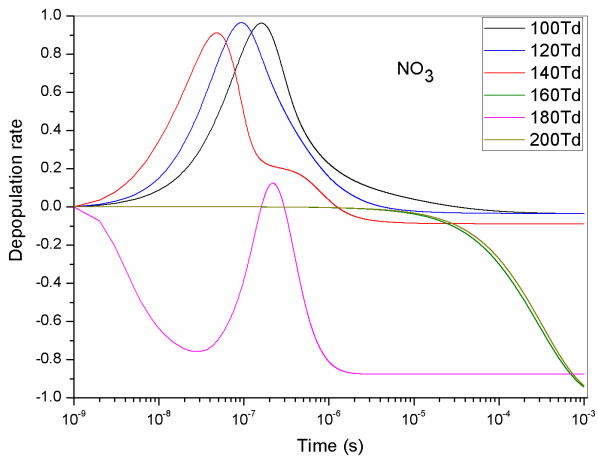


Fig. 12. Time evolution of depopulation rate of NO<sub>3</sub> specie in mixture N<sub>2</sub>/O<sub>2</sub>/H<sub>2</sub>O/CO<sub>2</sub> for different reduced electric fields [100-200 Td]

Figures 13 to 15 show some reactions which participate on creation of NO specie. We have described these reactions with their rate coefficient for varied values of reduced electrical fields (120, 140 and 180 Td). In our study

species that are actively concerned within the production of oxide nitrogen are N, N (<sup>2</sup>D), O<sub>2</sub>, NO<sub>3</sub><sup>-</sup>, O<sub>3</sub><sup>-</sup> and CO<sub>2</sub>. We notice that the evolution depends strongly on the increase of reduced electric field. Generally, the fractions of the energy transferred from charged to neutral particles via elastic and inelastic processes are given from a Boltzmann equation solution [29]. So, the fraction of energy lost during elastic, excitation and ionization processes in the same gas mixture depends on the electric reduced field. For example, at low values less than 120 Td, the energy loss is due to rotational and vibration collisions, where as for values more than 120 Td the energy loss is mainly due to electronic excitation and ionization collisions [21].

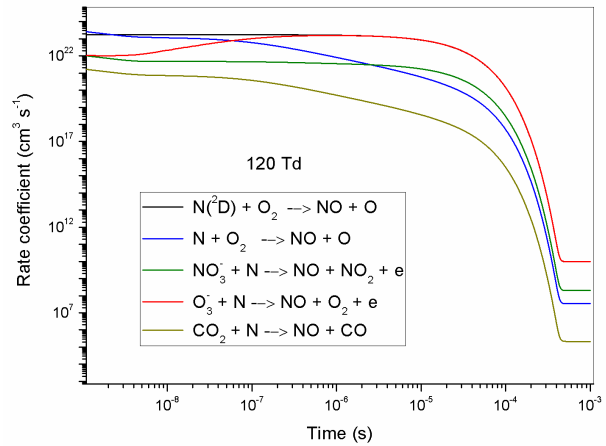


Fig. 13. Time evolution at 120 Td of rate coefficient with the following reactions: R41: N (<sup>2</sup>D) +O<sub>2</sub> → NO+O, R15: N+O<sub>2</sub> → NO+O, R39: NO<sub>3</sub>+ N→ NO + NO<sub>2</sub> + e, R24: O<sub>3</sub>+ N→ NO + O<sub>2</sub> + e, R45: CO<sub>2</sub> + N → NO + CO

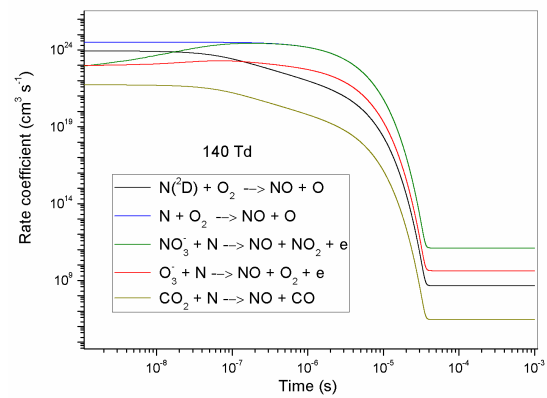


Fig. 14. Time evolution at 140 Td of rate coefficient with the following reactions: R41: N (<sup>2</sup>D) +O<sub>2</sub> → NO+O, R15: N+O<sub>2</sub> → NO+O, R39: NO<sub>3</sub>+ N→ NO + NO<sub>2</sub> + e, R24: O<sub>3</sub>+ N→ NO + O<sub>2</sub> + e, R45: CO<sub>2</sub> + N → NO + CO

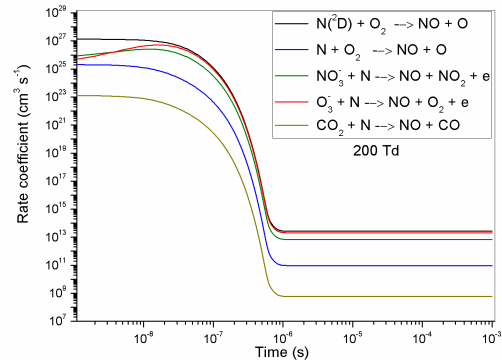


Fig. 15. Time evolution at 200 Td of rate coefficient with the following reactions:R41: N (<sup>2</sup>D) +O<sub>2</sub> → NO+O, R15: N+O<sub>2</sub> → NO+O, R39: NO<sub>3</sub>+ N→ NO + NO<sub>2</sub> + e, R24: O<sub>3</sub>+ N→ NO + O<sub>2</sub> + e, R45: CO<sub>2</sub> + N → NO + CO

#### 4. Conclusions

In this work, numerical studies were conducted to explore the evolution of the plasma discharge and its interaction with completely different completely different species involved in  $N_2/O_2/H_2O/CO_2$  mixed gas induced by negative corona discharge under different reduced electrical fields. Above all we tend to investigate the consequences of certain species on  $NO_x$  conversion. The results show two types of evolution, which depends strongly on the increase of reduced electric field:

(1) A reduction of dominant species in the mixture such as  $NO$ ,  $NO_2$  and  $NO_3$ . This reduction was obtained essentially on one hand through radical species  $OH$  and

$HO_2$ , and on the other hand through negative ions  $O_2^-$ ,  $O_3^-$  and  $O_4^-$ . We have found that the depopulation rate of  $NO$ ,  $NO_2$  and  $NO_3$  is substantially affected by the rise of reduced electric field as it grows from 100 Td to 200 Td. (2) A creation of other species such as  $HNO_3$ ,  $H$ ,  $CO$ , and  $N_2O_5$ . Finally, these results permit us to determine the vital role played by the reduced electric field on species evolution, and to higher perceive the various reaction processes affecting the  $NO_x$  concentration magnitude within the gas mixture.

This is an Open Access article distributed under the terms of the Creative Commons Attribution Licence



#### References

1. Y. P. Raizer, *J. Phys. D: Appl. Phys.*, 37, 851 (1991)
2. J. S. Hammer, *Plasma Sources Sci. Technol.*, 11, A196 (2002)
3. J. S. Chang, *Plasma Sources Sci. Technol.*, 17, 045004 (2008)
4. M. Laroussi, *IEEE Trans. Plasma Sci.*, 24, 1188 (1996)
5. M. Simek and M. Clupek, *J. Phys. D: Appl. Phys.*, 35, 1171 (2002)
6. B. Eliasson and U. Kogelschatz, *IEEE Trans. Plasma Sci.*, 19, 1063 (1991)
7. J. Chen and J. H. Davidson, *Plasma Chem. Plasma Process.*, 22, 495 (2002)
8. Y. S. Akishev, A. A. Deryugin, I. V. Kochetov, A. P. Napartovich, and N. I. Trushkin, *J. Phys. D: Appl. Phys.*, 26, 1630 (1993)
9. M. Laroussi, A. Fridman, P. Favia, and M. R. Wertheimer, *Plasma Process. Polym.*, 7, 193 (2010)
10. A. M. Pointu, A. Ricard, E. Odic, M. Ganciu, *Plasma Process. Polym.*, 5, 559 (2008)
11. C. C. Wang and S. J. Roy, *Appl. Phys.*, 106, 013310 (2009)
12. E. Moreau, *J. Phys. D: Appl. Phys.*, 40, 605 (2007)
13. G. Fridman, G. Friedman, A. Gutsol, A. B. Shekhter, V. N. Vasilets, and A. Fridman, *Plasma Processes and Polymers*, 5, 503 (2008)
14. Tendero C., Torche plasma micro-onde à la pression atmosphérique: application au traitement de surfaces métalliques *Ph.D. Université de Limoges*, France (2005)
15. L. Miao, S. Tanemura, H. Watanabe, Y. Mori, K. Kaneko and S. J. Toh, *Crystal Growth*, 260, 118 (2004)
16. F. Fresnet, G. Baravian, L. Magne, S. Pasquiers, C. Postel, V. Puech and A. Rousseau, *Plasma Sources Sci. Technol.* 11, 152 (2002)
17. M. Baeva, A. Pott and J. Uhlenbusch, *Plasma Sources Sci. Technol.* 11, 135 (2002)
18. B. Eliasson and U. Kogelschatz, *IEEE Trans. Plasma Sci.* 19, 1065 (1991)
19. B. M. Penetrante, J. N. m Bardsley, M. C. Hsiao, *Japan. J. Appl. Phys.* 36, 5007 (1997)
20. B. M. Penetrante and S. E. Schultheis (eds) Non-Thermal Plasma Techniques for Pollution Control parts A and B, *Springer*, Berlin (1993).
21. A. K. Ferouani, M. Lemerini and B. Liani, Numerical Modelling Chap 7, Edited by *Preep Miidla Croatia* 143-156 (2012)
22. W. Sun, B. Pashaie, S. Dhali and F. I. Honea, *J. Appl. Phys.* 79, 3438 (1996)
23. N. Spyrou, B. Held, R. Peyrous, Held, C. Manassis and P. Pignolet, *J. Phys. D: Appl. Phys.*, 25, 211 (1992)
24. Y. Creighton, Pulsed positive corona discharges: fundamental study and application to flue gas treatment *Ph.D. Technische University of Eindhoven*, Netherlands (1994)
25. J. Batina, F. Noël, S. Lachaud S, R. Peyrous and J. F. Loiseau, *J. Phys. D: Appl. Phys.*, 34, 1510 (2001)
26. R. Ono and T. Oda, *Japanese Journal of Applied Physics*, 43, 321 (2004)
27. O. Eichwald, M. Yousfi, A. Hennad A, and M. D. Benabdessadok, *J. Appl. Phys.*, 82 4781 (1997)
28. L. B. Loeb, Electrical Coronas, Their basic physical mechanism *Ph.D. Univ. of California Press*, Berkeley and Los Angeles (1965)
29. J. F. Loiseau, J. Batina, F. Noël, and R. Peyrous, *J. Phys. D: Appl. Phys.*, 35, 1020 (2002)
30. L. Zhao, K. Adamiak, *Journal of Electrostatics*, 63, 337 (2005)
31. A. Flitti and S. Pancheshnyi, *Eur. Phys. J. Appl. Phys.*, 45, 21001 (2009)
32. A. Haddouche, M. Lemerini. *Plasma Science and Technology*, 17, 589 (2015)
33. S. Katsuki, K. Tanaka, T. T. Fudamoto, *Japanese Journal of Applied Physics*, 45, 239 (2006)
34. I. A. Kossyi, A. Y. Kostinsky, A. A. Matveyev, and V. P. Silakov, *Plasma Sources Sci. Technol.*, 1, 207 (1992)
35. O. Eichwald, N. A. Guntoro, M. Yousfi and M. Benhenni, *J. Phys. D: Appl. Phys.*, 35, 439 (2002)
36. S. Nagaraja, V. Yangand and I. Adamovich, *J. Phys. D: Appl. Phys.*, 46, 155205 (2013)
37. J. S. Chang, *J. Aerosol. Sci.* 20, 1087 (1989)
38. Y. S. Mok and S. W. Ham, *Chem. Eng. Sci.*, 53, 1667 (1998)
39. R. Atkinson, D. L. Baulch, R. A. Coa, and J. Troe, *J. Phys. Chem. Ref. Data* 26, 521 (1997)
40. L. A. Rosocha, G. K. Anderson, L. A. Bechtold, J. J. Coogan, H. G. Heck, M. Kang, W.H. McCulla, R. A. Tennant, and P. J. Wantuck, Non-Thermal Techniques for Pollution Control: Part B, *Springer*, Berlin, 281-308 (1993)
41. Y. S. Mok, S. W. Ham, and I. S. Nam, *IEEE Trans. Plasma Sci.* 26, 1556 (1998)